

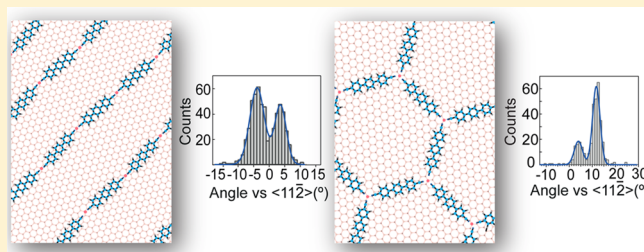
Competing Interactions in the Self-Assembly of NC-Ph₃-CN Molecules on Cu(111)

Giulia E. Pacchioni, Marina Pivetta,* and Harald Brune

Institute of Condensed Matter Physics, Ecole Polytechnique Fédérale de Lausanne (EPFL), CH-1015 Lausanne, Switzerland

Supporting Information

ABSTRACT: We report on low-temperature scanning tunneling microscopy and spectroscopy measurements on NC-Ph₃-CN molecules adsorbed at 300 K on a Cu(111) surface. Upon cooling, the molecules form chain and honeycomb structures, incorporating Cu adatoms supplied by the substrate as metal linkers. In these assemblies, the molecules align along two main directions, with a relative abundance that depends on the coordination number and on the bond length. We show spectroscopic data about the unoccupied molecular orbitals and investigate the patterns obtained by depositing different amounts of molecules. Comparison of these results with the ones obtained for NC-Ph₅-CN molecules on the same substrate enables us to establish a hierarchy of the different interaction forces at work in the system.



INTRODUCTION

Supramolecular chemistry at surfaces is a topic of widespread interest because low-dimensional architectures with specific functionalities can be created.^{1–4} A detailed understanding of the mechanism underlying the self-assembly of the various organic and metal–organic networks is important to realize the desired morphology, chemical composition, and eventually functionality. In this respect, regular porous networks are especially promising: They act as templates for the positioning of molecules or metal atoms and clusters onto well-defined sites within the cavities^{5–8} as well as on the ligand molecules.⁹ Moreover, depending on the metal atoms used for the coordination nodes, regular arrays of transition-metal^{10,11} or rare earth atoms¹² can be created.

Molecular adsorption and assembly are controlled by several competing interactions.^{13–16} For the case of metal–organic porous networks, there are the van der Waals forces between the organic molecules and the surface and the corrugation of this potential energy surface upon translation and rotation of the molecules. A second ingredient is the potential energy surface felt by the metal coordination atoms, that is, their preferred adsorption sites and their diffusion barriers. Finally, there are the bond angle, distance, and coordination number of the metal–organic coordination bond.

To shed light on the hierarchy of these energies, we report here on the self-assembly of NC-Ph₃-CN molecules on Cu(111). When deposited on the substrate kept at room temperature, upon cooling NC-Ph₃-CN molecules form chain and honeycomb structures and the molecules align with orientations that deviate from the crystallographic high symmetry directions of the surface. The comparison with the motifs formed by NC-Ph₅-CN molecules on the same substrate¹⁷ enables us to estimate which interaction dominates

in each case, depending on the number of phenyl rings in the system. To complement the characterization of the observed metal–organic structures, we report spectroscopic data for the molecular orbitals. Moreover, the dependence of the obtained structures on the molecular coverage is discussed.

EXPERIMENTAL METHODS

The Cu(111) surface was prepared by Ar⁺ sputtering (2 μA/cm², 800 eV, 20 min) and annealing (800 K, 20 min) cycles. NC-Ph₃-CN molecules¹¹ were evaporated from a molecular effusion cell at 145 °C on the substrate kept at room temperature (RT). The sample was then cooled to the scanning tunneling microscope (STM) measurement temperature of 5 K.¹⁸ The tunneling parameters are given in the Figure captions, and the modulation amplitudes for the spectroscopy measurements are peak-to-peak values.

We define one monolayer (ML) of molecules as the densest structure formed by NC-Ph₃-CN molecules on Cu(111), that is, the purely organic chevron pattern that is shown in the [Supporting Information](#). One ML corresponds to one molecule per 19 substrate atoms or 0.81 molecules/nm². The molecular coverage is determined by counting the molecules on many representative STM images; the deposition conditions are identical for all of the samples shown. For all samples except the ones in [Figure 6](#), the coverage is 0.30 ± 0.03 ML.

RESULTS AND DISCUSSION

For RT deposition and after cooling the sample to low temperature,¹⁷ we observe the coexistence of two metal–

Received: September 4, 2015

Revised: October 16, 2015

Published: October 19, 2015

organic structures: an arrangement of 1D chains and a honeycomb network.

Chains. A large-scale image showing the molecules arranged in parallel equidistant chains is displayed in Figure 1a. Two of

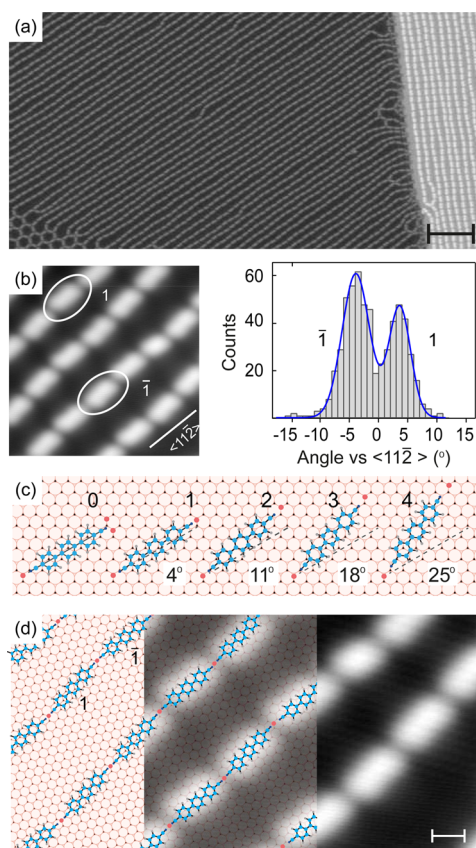


Figure 1. Metal–organic chains. (a) Large-scale STM image of two rotational chain domains (scale bar = 20 nm). (b) Close-up view showing the alternate orientation of the molecular axes with respect to the chain direction, labeled 1 and $\bar{1}$. Histogram: angular distribution of the molecular axes with respect to the chain direction $\langle 11\bar{2} \rangle$. The solid line is a double Gaussian fit to the data. (c) Different orientations of the molecular axes: 0 along $\langle 11\bar{2} \rangle$, 1, 2, 3, and 4 with the indicated angles with respect to the $\langle 11\bar{2} \rangle$ direction, represented as dashed line. Red dots are the Cu coordination adatoms supposed to be on fcc sites. (d) Close-up view accompanied by a model of the assembly (scale bar = 1 nm). Two molecules oriented in directions 1 and $\bar{1}$, respectively, are indicated. Tunneling parameters for all STM images: $V_t = -200$ mV, $I_t = 50$ pA.

the three rotational domains are visible, and the lower left corner shows a small domain of the honeycomb network that will be discussed in the following section. Closer inspection reveals that the chains are not perfectly straight. The close-up view of Figure 1b shows that the chains are aligned along the second nearest neighbor directions of the substrate, $\langle 11\bar{2} \rangle$; however, the molecules themselves deviate from this direction, as evidenced by the histogram of orientation angles of the molecular axes with respect to $\langle 11\bar{2} \rangle$, which shows two peaks at $\pm 4^\circ$. We label these directions 1 and $\bar{1}$, respectively. The wavy appearance of the resulting chains, also visible in the overview image, can thus be attributed to the alternance of 1 and $\bar{1}$ molecules.

Figure 1c illustrates the epitaxy of the molecules for the relevant orientations of the molecular axis. The first ingredient

to the total binding energy of the metal–organic structures is the registry of the molecule with the substrate. This part clearly favors alignment along $\langle 11\bar{2} \rangle$ because the distance between consecutive phenyl rings is, with 4.41 Å,¹¹ very close to the one between two Cu atoms in the $\langle 11\bar{2} \rangle$ directions, 4.43 Å.¹⁹ Hence this orientation allows all phenyl rings to occupy equivalent sites. Because benzene rings prefer to occupy the 3-fold hollow sites we assume that the phenyl rings do so, too.^{20,21} An additional argument for this adsorption geometry is that half the hydrogen atoms of the molecule can be located on their preferred fcc adsorption sites.^{22,23} Finally, in this configuration also the N atoms are on hollow sites, which were reported to be favorable on Ag(111).²⁴ The second part of the total energy comes from the positions of Cu adatoms and their bond distance and angle to the terminal carbonitrile groups. Individual Cu adatoms clearly favor fcc sites. DFT finds that the hcp sites are as unstable as the bridge sites,²⁵ which would favor the fcc site by the diffusion barrier that amounts to 40 ± 1 meV for that system;²⁶ in agreement, experiment observes exclusive occupation of fcc sites.²⁷ The bond between a metal atom and the carbonitrile group is strongly directional along the CN axis.²⁸ As illustrated in Figure 1c, the closest directions to $\langle 11\bar{2} \rangle$ allowing the molecule to have the two Cu adatoms in line with the molecular axis are the ones observed in the chains. They are labeled 1 and $\bar{1}$ and deviate from the high symmetric direction by $\pm 4^\circ$. This shows that for the molecules with three phenyl rings the directionality of the metal coordination bond and the registry of the metal atoms with the substrate dominate over the registry of the organic molecule. For five phenyl rings this balance is reversed, favoring alignment of the molecular axis.¹⁷ The other possible orientations allowing a straight node at each end form angles of 11, 18, and 25° with the second nearest neighbors directions (directions 2, 3, and 4, respectively) and are observed in the honeycomb network.

In Figure 1d we show a close-up view of the chains accompanied by the proposed model. Although Cu coordination adatoms are not imaged we infer their presence by comparison with the networks formed by NC-Ph₃-CN on the same substrate¹⁷ and from the fact that the measured CN-Cu bond length of 1.4 ± 0.1 Å is on the same order of the reported values of 1.6 to 1.9 Å.^{11,17,29,30} The model presented along with the image shows the alternating orientations of the molecular axes deviating by $\pm 4^\circ$ from the $\langle 11\bar{2} \rangle$ directions. Cu adatoms are represented with red dots and are found at every node. Minute amounts of shorter molecules are present as contaminants in the NC-Ph₃-CN powder. One such molecule, with two phenyl rings, is observed in the upper right corner of Figure 1d.

For the given molecular coverage of 0.30 ML, about half of the surface is covered with equidistant chains that are spaced by 2.08 ± 0.07 nm. The regular spacing of the chains hints toward the presence of a lateral repulsion between the molecules, as demonstrated by the fact that at lower coverages the chains are further apart from each other but still equidistant; see Figure 6b. The origin of this repulsive interaction could be a charge transfer to or from the substrate,³¹ while a surface-state mediated interaction can be excluded owing to the monotonic coverage dependence of the interchain distance. The rest of the surface is covered by the honeycomb network, which we will discuss now.

Honeycomb. We observe two types of honeycomb networks that coexist with the chains. The first is very regular and is shown in Figure 2, while the second involves more

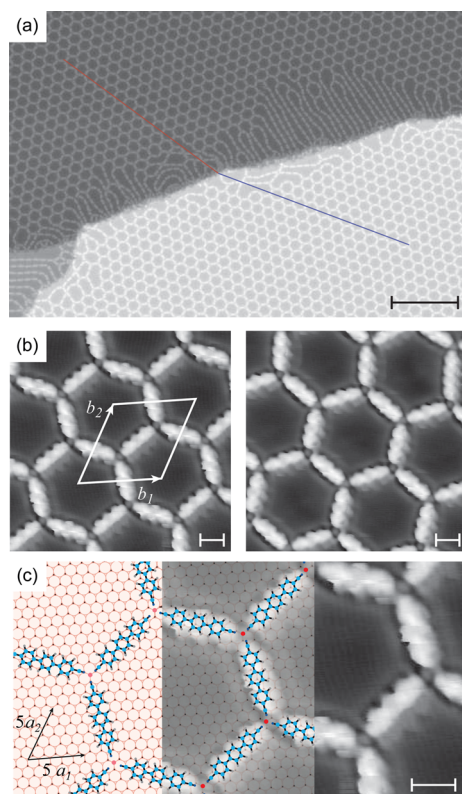


Figure 2. Regular honeycomb network. (a) Overview of two rotational domains of honeycomb network on two Cu(111) terraces separated by a double step ($V_t = -600$ mV, $I_t = 100$ pA, scale bar = 20 nm). (b) Close-up view of the two domains (scale bars = 1 nm). A CO-functionalized tip reveals intermolecular structure as well as the Cu coordination atoms. The unit cell is indicated ($V_t = -2$ mV, $I_t = 2$ nA). (c) Detail of the network and model, tunneling parameters as in panel b, scale bar = 1 nm.

variations between the honeycomb cells and is shown in Figure 3. The regular network exhibits two rotational domains forming an angle of 22° with respect to each other; see Figure 2a. A close-up view of each domain is shown in Figure 2b. These images were obtained with a CO-functionalized tip³² and clearly reveal the three phenyl rings of each molecule and the coordination adatoms. Each of the rotational domains involves molecules in directions 2 and $\bar{2}$, rotated by + or -11° from the $\langle 11\bar{2} \rangle$ directions, respectively. Figure 2c shows our model of one domain together with a high-resolution STM image. The unit cell for this network is

$$\begin{pmatrix} b_1 \\ b_2 \end{pmatrix} = \begin{pmatrix} 12 & 3 \\ -3 & 15 \end{pmatrix} \begin{pmatrix} a_1 \\ a_2 \end{pmatrix}$$

with $b_1 = b_2 = \sqrt{189} a = 3.51$ nm ($a_1 = a_2 = a = 2.56$ Å).

The irregular honeycomb network, presented in Figure 3a, involves in addition to the orientation 2 (70%) also the orientation 1 (30%) and very few orientations 3 and 4 as defects, as seen from the histogram in Figure 3b. Also in this case, two rotational domains are formed that are again symmetric with respect to the second nearest-neighbor directions of the substrate. The four molecular orientations differ not only by their alignment with respect to the substrate but also by the length of the CN-Cu bond. Assuming that the linker length does not change upon adsorption of NC-Ph₃-CN onto the Cu(111) surface, we find a growing surface projected

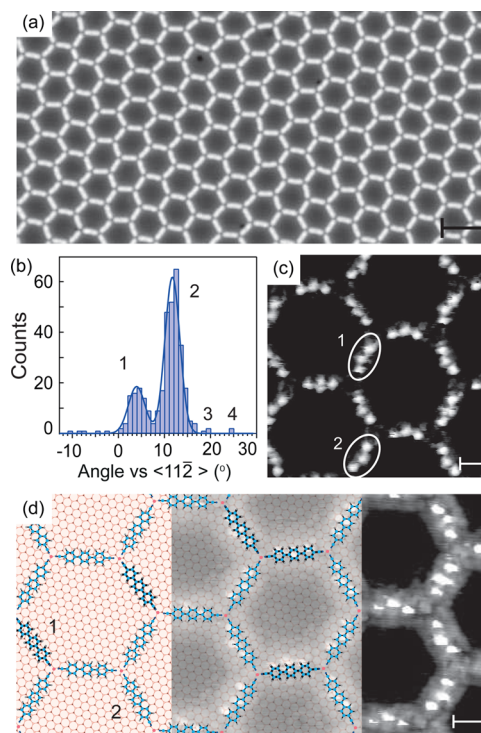


Figure 3. Irregular honeycomb network. (a) Overview of the network ($V_t = +20$ mV, $I_t = 200$ pA, scale bar = 5 nm). (b) Histogram of molecular axes angles with respect to $\langle 11\bar{2} \rangle$, for one rotational domain; solid line: double-Gaussian fit. (c) Small-scale image measured with a D₂-functionalized tip with molecules in orientations 1 and 2 highlighted. These molecules appear slightly bent owing to the tilt of the central phenyl ring ($V_t = -10$ mV, $I_t = 100$ pA, scale bar = 1 nm). (d) Detail of the network and structure model. Those molecules with orientation 1 are represented in bold, tunneling parameters as in panel c, scale bar = 1 nm.

bond length with increasing deviation from the second nearest-neighbor directions, with values of 1.4 ± 0.1 , 1.6 ± 0.1 , 1.9 ± 0.1 , and 2.3 ± 0.1 Å for the directions 1, 2, 3, and 4, respectively. The first three values are comparable to the bond length found for the same linkers with Co coordination adatoms on Ag(111) (1.6^{11} – 1.8 Å³⁰), for bipyridyl molecules coordinated by Cu atoms on Cu(100) (1.9 Å),²⁹ and for NC-Ph₃-CN molecules coordinated by Cu atoms on Cu(111) (1.9 Å).¹⁷ The last orientation implies an energetically less favorable very long distance between Cu and NC. We suggest that this difference in bond length has the major contribution to the total energy of the respective molecular orientations. To rationalize the fact that in the chains the favored orientation results in a shorter bond length compared with the one mostly found in the honeycomb, we observe that there is a clear trend linking a decreasing coordination number at the nodes and a shorter bond length. Reported values include 2.4 Å for NC-Ph₃-CN 5-fold coordinated to Ce adatoms on Ag(111),¹² 2.15 Å for TCNQ 4-fold coordinated to Mn atoms on Cu(100),³³ 1.9 Å for NC-Ph_n-CN 3-fold coordinated to Co atoms on Ag(111),³⁴ and the same value for NC-Ph₅-CN 3-fold coordinated to Cu atoms on Cu(111).⁷

A model for the irregular honeycomb pattern together with a high-resolution STM image measured with a D₂-terminated tip^{35,36} is shown in Figure 3d, with those molecules aligned along direction 1 represented in bold.

Upon closer inspection, the STM images reveal that NC-Ph₃-CN molecules have a slightly curved appearance. This effect is detected in STM images recorded with unfunctionalized tips; however, it is particularly prominent in images measured with a D₂-functionalized tip, as seen in Figure 3c,d. There is a direct relationship between the molecule orientation and its apparent curvature: Figure 3c reveals that molecules lying in directions 1 and 2, for example the ones in the two circles, have different apparent curvatures. Dicarbonitrile-polyphenyl molecules are known to exhibit an alternating tilt of consecutive phenyl rings, even when they are adsorbed at surfaces.³⁷ In the case of NC-Ph₃-CN, the central ring has a tilt angle with respect to the plane of the other two rings, and its value can change depending on the interaction with the underlying substrate, as was already reported for sexiphenyl molecules on Ag(111).³⁸ Thus, we ascribe the different apparent curvatures of the molecules aligned in directions 1 and 2 to a different tilt of the central phenyl ring. We note, moreover, that while for molecules in direction 2 the arc shape is observed for 93% of the ligands, molecules in direction 1 have a curved appearance in only 46% of the cases, and the curvature is less evident, indicating that in this case the tilt of the central phenyl ring is less pronounced or sometimes even absent. Notice that the relative tilt of phenyl rings was already identified as the cause for the zigzag appearance of dicarbonitrile-polyphenyl molecules.³⁷

Spectroscopy. Scanning tunneling spectroscopy (STS) was used to probe the unoccupied orbitals of molecules, both in the chains and in the honeycomb structure. The differential conductance spectra (dI/dV) acquired on different locations over a molecule in a chain are shown in Figure 4a. Each spectrum is the average of several spectra measured on equivalent locations of different molecules. The lowest unoccupied molecular orbital (LUMO) is extended over the whole molecule and has its maximum intensity on the central part of the ligand, slightly off-center (green line), and is situated

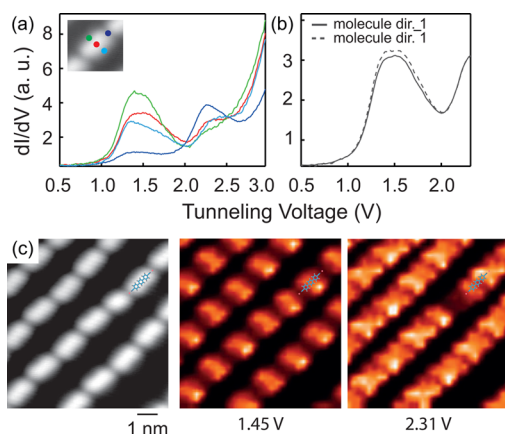


Figure 4. Spectroscopy on the chains. (a) dI/dV spectra acquired at the locations shown in the inset (red: center of the molecule, green: left side, light blue: right side, blue: node). From each spectrum we subtracted the signal acquired on the substrate. (b) dI/dV spectra measured above the center of molecules with orientations 1 and $\bar{1}$, respectively. (c) Topography and corresponding STS map at 1.45 and 2.31 V showing the LUMO and the LUMO+1 of the molecules, respectively. A molecular backbone is superimposed for comparison. Parameters for all spectra: set point $V_t = +500$ mV, $I_t = 10$ pA, and $V_{mod} = 20$ mV at 523 Hz. The maps were extracted from a grid of 32×32 dI/dV spectra.

at an energy of 1.45 eV. The LUMO+1, on the contrary, is localized at the molecular ends and at an energy of 2.30 eV (blue line). The LUMO+2 lies at an energy higher than the experimental limit of 3 eV, imposed by damage of the network at the corresponding voltages. In Figure 4c differential conductance maps at 1.45 and 2.31 V are shown along with the corresponding topographic (constant current) STM image. The presence of a shorter molecule, with only two phenyl rings, is particularly evident in the map representing the LUMO+1, where it appears dark. Surprisingly, these orbitals have a lateral extension far larger than the width of the molecule. (One molecular backbone is sketched for comparison.) In addition, in most molecules, the LUMO shows a higher intensity on one side. This effect is also seen in the honeycomb networks and will be discussed in detail further later. The extension of the LUMO over the whole molecular length and the localization of the LUMO+1 at molecular ends agree with a qualitative description of the electronic structure, considering the molecule as a linear chain of three benzene rings.³⁹ Figure 4b compares spectra acquired on the center of two molecules with the two most abundant orientations 1 and $\bar{1}$, respectively. There is no appreciable difference in the position and intensity of the LUMO, as expected for these two symmetrically equivalent orientations.

The spectra acquired over the molecules in the honeycomb network are presented in Figure 5a. As in the chains, the LUMO is located at the center of the molecule and has its highest intensity on one side of the molecular axis. The LUMO + 1 is also recognized; however, its maximum is just beyond the scanned voltage range. As illustrated in Figure 5b, molecules

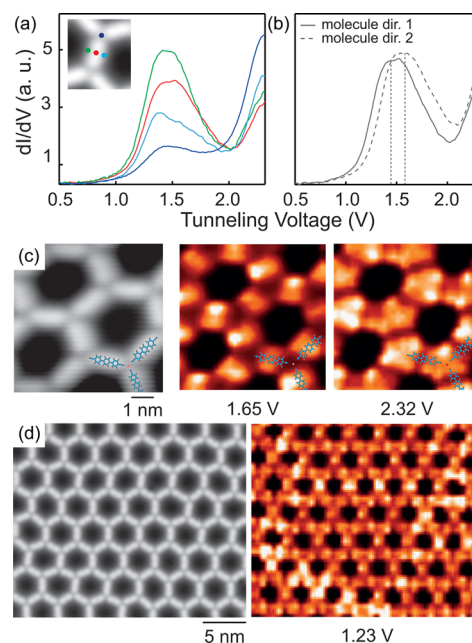


Figure 5. Spectroscopy on the honeycomb network. (a) dI/dV spectra acquired at the locations shown in the inset (red: center of the molecule, green: left side, light blue: right side, blue: node). (b) dI/dV spectra measured on the center of molecules with orientations 1 and 2, respectively. (c) Topography and corresponding STS maps at 1.65 and 2.32 V. Three molecular backbones are superimposed for comparison. (d) Topography and corresponding STS map at 1.23 V. Parameters for all spectra: set point $V_t = +500$ mV, $I_t = 10$ pA, and $V_{mod} = 20$ mV at 523 Hz.

oriented along direction 1 show the LUMO at 1.45 eV, consistent with the result obtained for ligands in the chains, while the LUMO of molecules lying in direction 2 is shifted upward, to 1.60 eV. Differential conductance maps recorded on a small area of the network are presented in Figure 5c along with the corresponding STM image. The first map is recorded at 1.65 V, thus close to the energy of the LUMO of molecules with orientation 2. Accordingly, these molecules appear bright while those with orientation 1 appear dark. In addition, one clearly sees that the LUMO of the molecules with orientation 2 has the highest intensity on one side. The second map, at 2.32 V, shows that the LUMO+1 is located on the ends of the molecule. It merges at the meeting point of three ligands, where it forms triangular-shaped bright features. Figure 5d shows a large scale dI/dV map recorded at 1.23 V, together with the topographic image. At this energy the spectra of molecules with orientation 1 are more intense than the ones of molecules with orientation 2, and thus the former can be easily identified from their bright color. This map reveals that, for geometrical reasons, the presence of one molecule in direction 1 tends to generate a row of ligands in that same direction.

We now address the question why the LUMO has its maximum intensity on one side of the molecule and why this is the case for many but not all of the ligands; see Figures 4c and 5c. The LUMO asymmetry with respect to the molecular axis is observed for 73% of the molecules, while for the remaining 27% the intensity of the orbital is highest at the center of the ligand and decreases symmetrically moving away from it to either side. For technical reasons, we cannot make a one-to-one correlation on a given molecule because spectra are measured with a tip that is optimized for spectroscopy and not for high-resolution imaging, making it difficult to resolve the curvature of the molecules. The fraction of molecules displaying the LUMO asymmetry is close to the fraction of molecules that appear bent in STM images, that is, 80%. Thus, we conclude that the tilt of the central phenyl ring that gives rise to the bent appearance is very likely also the cause of the LUMO asymmetry. The tilt angle depends on the position of the molecule with respect to the substrate. Large tilt angles cause an apparent curved shape and an asymmetry in the distribution of the LUMO due to the fact that the central ring is closer to the substrate on one side of the molecule.

Coverage Dependence. To get more insight into the competing interactions that decide on the metal–organic motifs, we performed measurements at molecular coverages below and above the one of 0.30 ML discussed so far. At 0.10 ± 0.01 ML the surface is entirely covered by an irregular network, Figure 6a. We can assimilate this pattern to widely spaced chains that frequently bend and meet to form 3-fold nodes. By increasing the coverage to 0.24 ± 0.03 ML, this pattern becomes denser, forming cavities that are smaller, approaching the dimension of the honeycomb cavities, Figure 6b. Domains of parallel chains coexist with this structure. Their separation is, with 2.47 ± 0.06 nm, larger than the one between the chains coexisting with the honeycomb structure at 0.30 ML. Finally, if the coverage is raised above 0.30 ML, namely, 0.40 ± 0.03 ML, a very dense pattern is obtained, with four-, five-, and six-fold nodes, Figure 6c. This network stems from the need of accommodating a higher number of molecules than in the honeycomb assembly. It is formed by introducing additional molecules in the honeycomb pattern and is strongly irregular. It is probably stabilized by a mixture of both metal-coordinated nodes and hydrogen bonds.

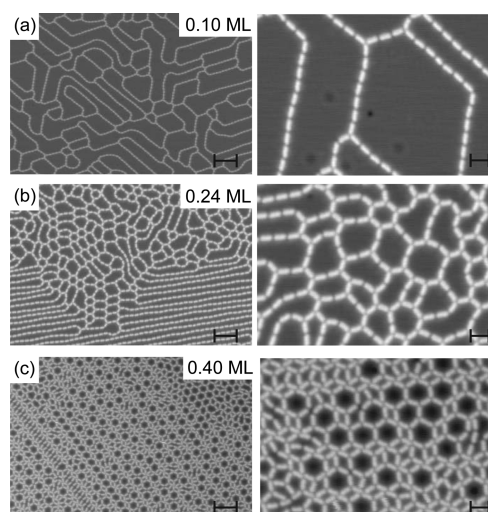


Figure 6. Coverage dependence. STM images of (a) 0.10 ± 0.01 ML, (b) 0.24 ± 0.03 ML, and (c) 0.40 ± 0.03 ML of NC-Ph₃-CN deposited at RT on Cu(111). For all images $V_t = -500$ mV and $I_t = 20$ pA; scale bars for overview images = 10 nm, scale bars for closeup views = 3 nm.

DISCUSSION

To elucidate the mechanisms underlying the self-assembly of linear polyphenyl molecules on Cu(111) we compare the results presented above with the ones reported for NC-Ph₃-CN molecules on the same substrate.¹⁷ Both NC-Ph₃-CN and NC-Ph₅-CN have an almost perfect epitaxial match when they are oriented along the $\langle 11\bar{2} \rangle$ directions of the Cu(111) surface. Both molecules, upon deposition on the substrate kept at room temperature, form coexisting honeycomb and chain structures; however, the molecular alignment is different: While NC-Ph₃-CN adsorbs with the orientations previously described, NC-Ph₅-CN aligns along the $\langle 11\bar{2} \rangle$ directions. We explain the origin of these different orientations in terms of competition between the interaction with the substrate, favoring the alignment along the second nearest-neighbor directions, and the one with the adatoms, favoring a configuration with both atoms right in front of the molecular ends and at a favorable distance. The longer molecule, with its 5 phenyl rings and 20 H atoms, has its most stable configuration when it optimizes the adsorption geometry with respect to the substrate, while the shorter molecule favors the straight bond at both ends. For these shorter molecules the alignment along the $\langle 11\bar{2} \rangle$ directions is never observed upon deposition at RT. On the contrary, upon deposition on the substrate kept at a lower temperature, the reduced availability of Cu coordination adatoms leads to the formation of patterns with half of the nodes metal-coordinated and half purely organic and assemblies with all nodes purely organic. In these structures, where there is an adatom only at one end of the molecule or no adatoms at all, the adsorption energy and the bond configuration can be optimized at the same time and NC-Ph₃-CN are oriented along $\langle 11\bar{2} \rangle$.

As a consequence of the different orientations of the molecules, the structures formed by the two ligands have some features in common but that have different origins. For example, both molecules form chains with a wavy appearance; however, the reason behind the waviness is not the same for the two ligands. In the case of NC-Ph₃-CN it is a consequence of the alternance of molecules with different orientations, while for the longer molecules it originates from the fact that the Cu

coordination atom is straight in front of the molecule at one end and laterally displaced at the other.¹⁷ As for the honeycomb network, in both cases two domains are formed, but for NC-Ph₃-CN they are rotational domains, while for NC-Ph₅-CN they are chiral domains, originating from the chiral nature of the nonaligned nodes.¹⁷ It has been reported that linear molecules differing only by the number of their constituent units can form structures with different stabilities and geometric properties depending on their commensurability with the substrate.²⁹ In our case, however, the long and the short molecules have the same almost perfect epitaxial coincidence with the surface. The differences in the patterns they form on the substrate have their origin in the different interactions that prevail in the two cases.

Finally, we compare the observed motifs with the metal–organic networks formed by the same two molecules on a Ag(111) surface.^{11,30} In that case, Co adatoms were codeposited with the molecules to provide coordination centers. A honeycomb network is obtained for both ligands. NC-Ph₃-CN molecules form distinct domains with the molecules aligned along the first or second nearest neighbors directions, respectively, while the orientation of NC-Ph₅-CN is not discussed. Coordination two is not observed. In the case of Ag(111) the registry between molecules and substrate is not matching as with Cu(111), and the Co atoms can occupy both the fcc and hcp sites.³⁴ This explains the different molecular orientations observed on this substrate compared with the ones we reported in this paper.

CONCLUSIONS

In conclusion, NC-Ph₃-CN molecules deposited on Cu(111) at RT form upon cooling chain and honeycomb structures that coexist. Unlike the NC-Ph₅-CN molecules, which align along the second nearest neighbor directions of the substrate, the molecules with three phenyl rings are oriented along two main directions deviating from the high symmetry ones and having a relative probability that depends on the resulting bond length between CN end group and Cu coordination atom. We explain the different behavior of the two molecules through the interplay between the gain in energy obtained by forming a straight CN-Cu bond with the right length and the one given by having the phenyl rings and hydrogen and nitrogen atoms placed on favorable adsorption sites on the surface. In the case of NC-Ph₃-CN the directionality of the metal coordination bond and the registry of the metal atoms with the substrate dominate over the registry of the molecule, while for NC-Ph₅-CN this balance is inverted. We also investigate the properties of the LUMO and LUMO+1 for the two networks, demonstrating that the different molecular orientations influence the energy of these orbitals. Moreover, the central phenyl ring of the molecules has a tilt that depends on the molecular orientation, giving rise to distinctive appearances of molecules and to an asymmetry in the spatial distribution of the LUMO across them. As a last point, we showed the networks that are obtained upon changing the molecular coverage.

ASSOCIATED CONTENT

Supporting Information

The Supporting Information is available free of charge on the ACS Publications website at DOI: 10.1021/acs.jpcc.5b08644.

Chevron pattern formed upon molecular deposition on the substrate kept at 190 K. (PDF)

AUTHOR INFORMATION

Corresponding Author

*E-mail: marina.pivetta@epfl.ch.

Notes

The authors declare no competing financial interest.

ACKNOWLEDGMENTS

We thank the Swiss National Science Foundation for financial support.

REFERENCES

- (1) Barth, J. V. Molecular Architectonic on Metal Surfaces. *Annu. Rev. Phys. Chem.* **2007**, *58*, 375–407.
- (2) Kudernac, T.; Lei, S. B.; Elemans, J. A. A. W.; De Feyter, S. Two-Dimensional Supramolecular Self-Assembly: Nanoporous Networks on Surfaces. *Chem. Soc. Rev.* **2009**, *38*, 402–421.
- (3) Elemans, J.; Lei, S.; De Feyter, S. Molecular and Supramolecular Networks on Surfaces: From Two-Dimensional Crystal Engineering to Reactivity. *Angew. Chem., Int. Ed.* **2009**, *48*, 7298–7332.
- (4) Bartels, L. Tailoring Molecular Layers at Metal Surfaces. *Nat. Chem.* **2010**, *2*, 87–95.
- (5) Stöhr, M.; Wahl, M.; Spillmann, H.; Gade, L. H.; Jung, T. A. Lateral Manipulation for the Positioning of Molecular Guests within the Confinements of a Highly Stable Self-Assembled Organic Surface Network. *Small* **2007**, *3*, 1336–1340.
- (6) Cheng, Z.; Wyrick, J.; Luo, M.; Sun, D.; Kim, D.; Zhu, Y.; Lu, W.; Kim, K.; Einstein, T. L.; Bartels, L. Adsorbates in a Box: Titration of Substrate Electronic States. *Phys. Rev. Lett.* **2010**, *105*, 066104.
- (7) Pivetta, M.; Pacchioni, G. E.; Schlickum, U.; Barth, J. V.; Brune, H. Formation of Fe Cluster Superlattice in a Metal–Organic Quantum-Box Network. *Phys. Rev. Lett.* **2013**, *110*, 086102.
- (8) Nowakowska, S.; Wäckerlin, A.; Kawai, S.; Ivas, T.; Nowakowski, J.; Fatayer, S.; Wäckerlin, C.; Nijs, T.; Meyer, E.; J, B.; et al. Interplay of Weak Interactions in the Atom-by-Atom Condensation of Xenon within Quantum Boxes. *Nat. Commun.* **2015**, *6*, 6071.
- (9) Decker, R.; Schlickum, U.; Klappenberger, F.; Zoppellaro, G.; Klyatskaya, S.; Ruben, M.; Barth, J. V.; Brune, H. Using Metal–Organic Templates to Steer the Growth of Fe and Co Nanoclusters. *Appl. Phys. Lett.* **2008**, *93*, 243102.
- (10) Stepanow, S.; Lin, N.; Payer, D.; Schlickum, U.; Klappenberger, F.; Zoppellaro, G.; Ruben, M.; Brune, H.; Barth, J. V.; Kern, K. Surface-Assisted Assembly of 2D Metal–Organic Networks that Exhibit Unusual Threefold Coordination Symmetry. *Angew. Chem., Int. Ed.* **2007**, *46*, 710–713.
- (11) Schlickum, U.; Decker, R.; Klappenberger, F.; Zoppellaro, G.; Klyatskaya, S.; Ruben, M.; Silanes, I.; Arnau, A.; Kern, K.; Brune, H.; et al. Metal–Organic Honeycomb Nanomeshes with Tunable Cavity Size. *Nano Lett.* **2007**, *7*, 3813–3817.
- (12) Urgel, J. I.; Ecija, D.; Auwärter, W.; Papageorgiou, A. C.; Seitsonen, A. P.; Vijayaraghavan, S.; Joshi, S.; Fischer, S.; Reichert, J.; Barth, J. V. Five-Vertex Lanthanide Coordination on Surfaces: a Route to Sophisticated Nanoarchitectures and Tessellations. *J. Phys. Chem. C* **2014**, *118*, 12908–12915.
- (13) Cañas-Ventura, M. E.; Ait-Mansour, K.; Ruffieux, P.; Rieger, R.; Müllen, K.; Brune, H.; Fasel, R. Complex Interplay and Hierarchy of Interactions in Two-Dimensional Supramolecular Assemblies. *ACS Nano* **2011**, *5*, 457–469.
- (14) Chapman, C. R. L.; Ting, E. C.; Kereszti, A.; Paci, I. Self-Assembly of Cysteine Dimers at the Gold Surface: a Computational Study of Competing Interactions. *J. Phys. Chem. C* **2013**, *117*, 19426–19435.
- (15) Sirtl, T.; Schlögl, S.; Rastgoo-Lahrood, A.; Jelic, J.; Neogi, S.; Schmittel, M.; Heckl, W. M.; Reuter, K.; Lackinger, M. Control of Intermolecular Bonds by Deposition Rates at Room Temperature: Hydrogen Bonds Versus Metal Coordination in Trinitrile Monolayers. *J. Am. Chem. Soc.* **2013**, *135*, 691–695.

- (16) Gottardi, S.; Müller, K.; Moreno-López, J. C.; Yildirim, H.; Meinhardt, U.; Kivala, M.; Kara, A.; Stöhr, M. Cyano-Functionalized Triarylaminates on Au(111): Competing Intermolecular Versus Molecule/Substrate Interactions. *Adv. Mater. Interfaces* **2014**, *1*, 1300025.
- (17) Pivetta, M.; Pacchioni, G. E.; Fernandes, E.; Brune, H. Temperature-Dependent Self-Assembly of NC-Ph₃-CN Molecules on Cu(111). *J. Chem. Phys.* **2015**, *142*, 101928.
- (18) Gaisch, R.; Gimzewski, J. K.; Reihl, B.; Schlittler, R. R.; Tschudy, M.; Schneider, W. D. Low-Temperature Ultra-High Vacuum Scanning Tunneling Microscope. *Ultramicroscopy* **1992**, *42–44*, 1621–1626.
- (19) Ashcroft, N.; Mermin, N. *Solid State Physics*; Saunders College: Philadelphia, 1976.
- (20) Chwee, T. S.; Sullivan, M. B. Adsorption Studies of C₆H₆ on Cu(111), Ag(111), and Au(111) within Dispersion Corrected Density Functional Theory. *J. Chem. Phys.* **2012**, *137*, 134703.
- (21) Reckien, W.; Eggers, M.; Bredow, T. Theoretical Study of the Adsorption of Benzene on Coinage Metals. *Beilstein J. Org. Chem.* **2014**, *10*, 1775–1784.
- (22) Spencer, M. J. S.; Nyberg, G. L. DFT Modelling of Hydrogen on Cu(110)- and (111)-type Clusters. *Mol. Simul.* **2002**, *28*, 807–825.
- (23) Feibelman, P. J.; Hamann, D. R. Theory of H Bonding and Vibration on Close-Packed Metal Surfaces. *J. Vac. Sci. Technol., A* **1987**, *5*, 424–426.
- (24) Kühne, D.; Klappenberger, F.; Decker, R.; Schlickum, U.; Brune, H.; Klyatskaya, S.; Ruben, M.; Barth, J. V. Self-Assembly of Nanoporous Chiral Networks with Varying Symmetry from Sexiphenyl-Dicarbonitrile on Ag(111). *J. Phys. Chem. C* **2009**, *113*, 17851–17859.
- (25) Bogicevic, A.; Ovesson, S.; Hyldgaard, P.; Lundqvist, B. I.; Brune, H.; Jennison, D. R. Nature, Strength, and Consequences of Indirect Adsorbate Interactions on Metals. *Phys. Rev. Lett.* **2000**, *85*, 1910.
- (26) Knorr, N.; Brune, H.; Epple, M.; Hirstein, A.; Schneider, M. A.; Kern, K. Long-Range Adsorbate Interactions Mediated by a Two-Dimensional Electron Gas. *Phys. Rev. B: Condens. Matter Mater. Phys.* **2002**, *65*, 115420.
- (27) Repp, J.; Meyer, G.; Rieder, K.-H.; Hyldgaard, P. Site Determination and Thermally Assisted Tunneling in Homogenous Nucleation. *Phys. Rev. Lett.* **2003**, *91*, 206102.
- (28) Abdurakhmanova, N.; Floris, A.; Tseng, T.-C.; Comisso, A.; Stepanow, S.; De Vita, A.; Kern, K. Stereoselectivity and Electrostatics in Charge-transfer Mn- and Cs-TCNQ₄ Networks on Ag(100). *Nat. Commun.* **2012**, *3*, 940.
- (29) Tait, S. L.; Langner, A.; Lin, N.; Stepanow, S.; Rajadurai, C.; Ruben, M.; Kern, K. One-Dimensional Self-Assembled Molecular Chains on Cu(100): Interplay between Surface-Assisted Coordination Chemistry and Substrate Commensurability. *J. Phys. Chem. C* **2007**, *111*, 10982–10987.
- (30) Schlickum, U.; Klappenberger, F.; Decker, R.; Zoppellaro, G.; Klyatskaya, S.; Ruben, M.; Kern, K.; Brune, H.; Barth, J. V. Surface-Confined Metal-Organic Nanostructures from Co-directed Assembly of Linear Terphenyl-Dicarbonitrile Linkers on Ag(111). *J. Phys. Chem. C* **2010**, *114*, 15602–15606.
- (31) Tomba, G.; Stengel, M.; Schneider, W.-D.; Baldereschi, A.; De Vita, A. Supramolecular Self-Assembly Driven by Electrostatic Repulsion: The 1D Aggregation of Rubrene Pentagons on Au(111). *ACS Nano* **2010**, *4*, 7545–7551.
- (32) Kichin, G.; Weiss, C.; Wagner, C.; Tautz, F. S.; Temirov, R. Single Molecule and Single Atom Sensors for Atomic Resolution Imaging of Chemically Complex Surfaces. *J. Am. Chem. Soc.* **2011**, *133*, 16847–16851.
- (33) Tseng, T.-C.; Lin, C.; Shi, X.; Tait, S. L.; Liu, X.; Starke, U.; Lin, N.; Zhang, R.; Minot, C.; Van Hove, M. A.; et al. Two-Dimensional Metal-Organic Coordination Networks of Mn-7,7,8,8-tetracyanoquinodimethane Assembled on Cu(100): Structural, Electronic, and Magnetic Properties. *Phys. Rev. B: Condens. Matter Mater. Phys.* **2009**, *80*, 155458.
- (34) Kühne, D.; Klappenberger, F.; Decker, R.; Schlickum, U.; Brune, H.; Klyatskaya, S.; Ruben, M.; Barth, J. V. High-Quality 2D Metal-Organic Coordination Network Providing Giant Cavities within Mesoscale Domains. *J. Am. Chem. Soc.* **2009**, *131*, 3881–3883.
- (35) Temirov, R.; Soubatch, S.; Neucheva, O.; Lassise, A. C.; Tautz, F. S. A Novel Method Achieving Ultra-High Geometrical Resolution in Scanning Tunneling Microscopy. *New J. Phys.* **2008**, *10*, 053012.
- (36) Weiss, C.; Wagner, C.; Kleimann, C.; Rohlfing, M.; Tautz, F. S.; Temirov, R. Imaging Pauli Repulsion in Scanning Tunneling Microscopy. *Phys. Rev. Lett.* **2010**, *105*, 086103.
- (37) Klappenberger, F.; Kühne, D.; Marschall, M.; Neppl, S.; Krenner, W.; Nefedov, A.; Strunskus, T.; Fink, K.; Wöll, C.; Klyatskaya, S.; et al. Uniform π -system Alignment in Thin films of Template-Grown Dicarbonitrile-Oligophenyls. *Adv. Funct. Mater.* **2011**, *21*, 1631–1642.
- (38) Hla, S.-W.; Braun, K.-F.; Wassermann, B.; Rieder, K.-H. Controlled Low-Temperature Molecular Manipulation of Sexiphenyl Molecules on Ag(111) using Scanning Tunneling Microscopy. *Phys. Rev. Lett.* **2004**, *93*, 208302.
- (39) Brocorens, P.; Zojer, E.; Cornil, J.; Shuai, Z.; Leising, G.; Müllen, K.; Brédas, J. Theoretical Characterization of Phenylene-Based Oligomers, Polymers, and Dendrimers. *Synth. Met.* **1999**, *100*, 141–162.